DOI: 10.1534/genetics.110.117655

Trivalent Arsenic Inhibits the Functions of Chaperonin Complex

Xuewen Pan,*,†,[1] Stefanie Reissman,‡ Nick R. Douglas,‡ Zhiwei Huang,† Daniel S. Yuan,* Xiaoling Wang,* J. Michael McCaffery,§ Judith Frydman‡ and Jef D. Boeke*,[1]

**Department of Molecular Biology and Genetics and The High Throughput Biology Center, The Johns Hopkins University School of Medicine, Baltimore, Maryland 21205, †Verna and Marrs McLean Department of Biochemistry and Molecular Biology and Department of Molecular and Human Genetics, Baylor College of Medicine, Houston, Texas 77030, ‡Department of Biological Sciences, Bio-X Program and Cancer Biology Program, Stanford University, Stanford, California 94305 and §Department of Biology and Integrated Imaging Center, The Johns Hopkins University, Baltimore, Maryland 21218*

Manuscript received April 10, 2010
Accepted for publication July 14, 2010

ABSTRACT

The exact molecular mechanisms by which the environmental pollutant arsenic works in biological systems are not completely understood. Using an unbiased chemogenomics approach in *Saccharomyces cerevisiae*, we found that mutants of the chaperonin complex TRiC and the functionally related prefoldin complex are all hypersensitive to arsenic compared to a wild-type strain. In contrast, mutants with impaired ribosome functions were highly arsenic resistant. These observations led us to hypothesize that arsenic might inhibit TRiC function, required for folding of actin, tubulin, and other proteins postsynthesis. Consistent with this hypothesis, we found that arsenic treatment distorted morphology of both actin and microtubule filaments. Moreover, arsenic impaired substrate folding by both bovine and archaeal TRiC complexes *in vitro*. These results together indicate that TRiC is a conserved target of arsenic inhibition in various biological systems.

ARSENIC is a ubiquitous environmental pollutant that causes severe health problems in humans. It is also used as an effective therapeutic agent against various diseases and infections. Using advanced genomic tools in the model organism yeast and biochemical experiments, we demonstrated that arsenic disturbs functions of the chaperonin complex required for proper folding and maturation of a large number of proteins. This mechanism of action by arsenic is conserved in various biological systems ranging from archaeal bacteria to mammals. Such an understanding should help in exploring possible ways to overcome toxic effects caused by exposure to arsenic.

Trivalent inorganic arsenic is among the most significant environmental hazards affecting the health of millions of people worldwide (Nordstrom 2002). Particularly, inorganic trivalent arsenic [As(III)] in underground drinking water and some mining environments is recognized as the cause of various cancers affecting the skin, lung, urinary tract, bladder, liver, and kidney (Tapio and Grosche 2006), as well as being implicated in several other disorders such as diabetes, hypertension, neuropathy, and vascular diseases (Tseng 2004). Interestingly, As(III) is also an effective therapeutic agent against cancer and human pathogens. A number of models have been proposed to explain the biological effects of As(III), including stimulation of reactive oxygen species (ROS) production (Miller *et al.* 2002; Tapio and Grosche 2006) and inhibition of tubulin polymerization (Ramirez *et al.* 1997; Li and Broome 1999). However, exactly how As(III) disturbs biological systems is still not clear.

The eukaryotic chaperonin TRiC (TCP1-ring complex, also called CCT) is a ~900-kDa complex consisting of two apposed heterooligomeric protein rings. Each ring, constituted by eight homologous subunits (encoded by the essential *CCT1–CCT8* genes in budding yeast), contains a central cavity in which unfolded polypeptide substrates attain a properly folded state in an ATP-requiring reaction (Bukau and Horwich 1998; Gutsche *et al.* 1999). TRiC is required for the proper folding of an important subset of cytosolic proteins, including cytoskeleton components, cell cycle regulators, and tumor suppressor proteins (Spiess *et al.* 2004). Some of these protein substrates are themselves encoded by essential genes; thus TRiC is indispensable for eukaryotic cell survival. Many TRiC substrates are subunits of oligomeric complexes and their assembly into functional multisubunit complexes also requires TRiC (Spiess *et al.* 2004). Assembly of such macromolecular complexes in some cases eliminates the accumulation of toxic subunits such as free β-tubulin molecules, which can bind to γ-tubulin and thereby

Supporting information is available online at http://www.genetics.org/cgi/content/full/genetics.110.117655/DC1.

The microarray data were submitted to GEO (accession no. GSE5973).

[1]*Corresponding authors:* 733 North Broadway, Room 339, Baltimore, MD 21205. Email: jboeke@jhmi.edu; and Department of Biochemistry, BCM 125, Houston, TX 77030. Email: xuewenp@bcm.tmc.edu

disrupt the formation of mitotic spindles in the yeast *S. cerevisiae* (Archer *et al.* 1995). Folding of yeast actin, α-tubulin, and β-tubulin and their oligomerization require TRiC and GimC (also known as prefoldin), a nonessential protein complex of six distinct but structurally related subunits of 13–23 kDa (Geiser *et al.* 1997; Vainberg *et al.* 1998). Mutational loss of GimC function substantially reduces actin and tubulin folding efficiency although it does not cause obvious growth defects in yeast. However, deletion of various GimC subunits strongly reduces the viability of conditional-lethal alleles of TRiC subunits under permissive conditions (Siegers *et al.* 1999).

To elucidate the mechanisms of inorganic As(III)'s action(s) in a eukaryotic system, we first took an unbiased functional chemogenomics approach in yeast to systematically probe for the genetic determinants of arsenic sensitivity. These genetic and subsequent biochemical results point to the conclusion that As(III) inhibits the yeast TRiC complex. This mechanism of action is apparently conserved because the activities of both a mammalian TRiC complex and an archaeal TRiC-like chaperonin are significantly inhibited by arsenic *in vitro*. Given that mammalian TRiC and some of its substrates are implicated in tumor suppression, angiogenesis, and neuropathy (Lee *et al.* 2003; Spiess *et al.* 2004; Bouhouche *et al.* 2006), TRiC is likely an important protein mediator of As(III)'s effects on human health.

MATERIALS AND METHODS

Profiling of the sensitivity of genome-wide deletion mutants to arsenic and individual validation were carried out as described in supporting information, File S1. As_2O_3 (Sigma-Aldrich, St. Louis, MO) was first dissolved in NaOH as a 400-mm stock solution of sodium arsenite.

Yeast strains and plasmids: Individual yeast deletion mutant strains used in this study were all obtained or derived from the yeast knockout mutants constructed by the Saccharomyces Genome Deletion Project (Giaever *et al.* 1999). The DAmP alleles of *TUB2*, *CCT1*, and *CCT2* were obtained from Open Biosystems (Breslow *et al.* 2008). The Cdc55p-3HA expression strain was a gift from Katja Siegers. Plasmids expressing *ACT1* and *TUB2* from a centromere-based plasmid were constructed by *in vivo* homologous recombination into YCplac33 (*CEN* and *URA3*) (Gietz and Sugino 1988). The *CCT1–CCT7*, *TUB1*, and *TUB3* overexpression plasmids were similarly constructed into YEplac195 (2 μ, *URA3*) (Gietz and Sugino 1988). Either YCplac33 or YEplac195 was used as the vector control.

Immunofluorescence: A 100-ml culture of the wild-type diploid yeast BY4743**a**/α was grown in YPD at 30° until mid-log phase and split. Sodium arsenite was added into one part of the culture at a final concentration of 1 mm. The other part served as a nontreatment control. Both were incubated at 30° for 3 additional hr. Immunofluorescence analyses of actin and microtubule morphology were performed as previously described (Rieder *et al.* 1996). Actin was stained with rhodamine-phalloidin and microtubule with an anti-α–tubulin antibody.

Immunoprecipitation and Western blotting: The yeast strain expressing Cdc55p–3HA was grown in 100 ml YPD at 30° until mid-log phase. The culture was split and sodium arsenite was added into one aliquot at a final concentration of 1 mm. The other aliquot served as a nontreatment control. Both were subsequently incubated at 30° for 1 hr before cells were harvested. Cell homogenization and immunoprecipitation were carried out essentially as described (Pan and Heitman 2002). An anti HA and anti-actin antibody were used to immunoprecipitate Cdc55p–3HA and actin, respectively. Cdc55p–3HA, actin and TRiC on the Western blots were detected with anti-HA, anti-actin, and anti-Cct5p antibodies.

***In vitro* actin folding assay:** The actin-folding assay was carried out as described by Frydman and Hartl (1996). Briefly, 0.25 μm TRiC was incubated in buffer A [20 mm Hepes-KOH (pH 7.5), 100 mm KOAc, 5 mm $MgCl_2$, 1 mm DTT, 10% glycerol, and 1% PEG 8000]. Subsequently [^{35}S]-actin, which was denatured in 6 m guanidine/HCl, was rapidly diluted 1:100 to a final concentration of 30 μm into the reaction mix. After incubation for 10 min at 4° and centrifugation at 14,000 × *g* for 10 min to remove aggregated actin, the reaction was supplemented with 1 mm ATP and incubated for 40 min at 30° to allow time for ATP-dependent actin refolding by the chaperonin. A total of 1 mm arsenite was added as indicated in the figure. Generation of native [^{35}S]-actin was determined by native gel electrophoresis using folded [^{35}S]-actin as a control as described previously (Frydman and Hartl 1996). The gel was exposed on a phosphor storage screen (Kodak) and scanned in a Typhoon 9410 imager (GE Healthcare).

Archaeal chaperonin folding assays: Purification of the archaeal chaperonin from Mm-Cpn was carried out by conventional chromatography essentially as described (Kusmierczyk and Martin 2003). Rhodanese folding by the archaeal chaperonin Mm-Cpn was assayed as described (Weber and Hayer-Hartl 2000). In brief, 0.25 μm protein was incubated in Cpn-buffer supplemented with 20 mm sodium thiosulfate. Purified rhodanese was denatured in 6 m guanidinium/HCl containing 5 mm DTT and rapidly diluted 1:100 to a final concentration of 30 μm into the reaction mix. After incubation for 5 min at 37°, the reaction was started by addition of 2 mm ATP and allowed to proceed for 50 min at 37°. To detect the presence of refolded rhodanese, 10 μl of the reaction was withdrawn and applied to a rhodanese activity assay performed as described (Weber and Hayer-Hartl 2000).

RESULTS

Mutants of the chaperonin pathway are As(III) hypersensitive: Haploinsufficiency of a target gene could lead to increased sensitivity to the cognate antiproliferation cytotoxin or drug (Giaever *et al.* 1999; Lum *et al.* 2004). To probe molecular mechanisms of As(III) actions in yeast, we investigated As(III) sensitivity of genome-wide heterozygous diploid yeast knockout (YKO) mutants using a TAG array-based analysis (Giaever *et al.* 1999; Lum *et al.* 2004) followed by individual validation. We found that 33 heterozygous diploid YKOs were significantly more sensitive than an isogenic wild-type strain to 450 μm sodium arsenite (Figure 1A and Table S1). Because As(III) completely inhibits yeast cell growth at higher concentrations, we reasoned that it might inactivate at least one essential protein or protein complex. A total of 15 of these 33 As(III)-hypersensitive mutants were heterozygous for essential genes, including five (*CCT1*, *CCT4*, *CCT5*, *CCT7*, and *CCT8*) encoding subunits of the TRiC complex and two more (*SPC97*

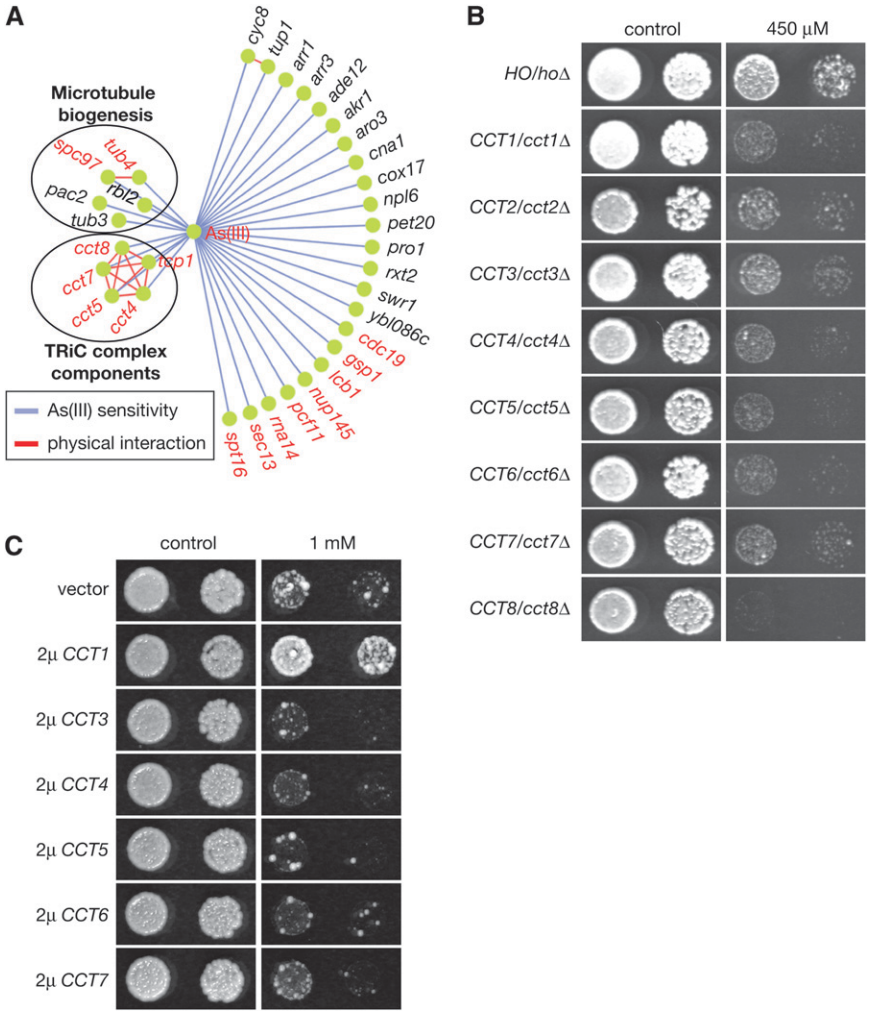

FIGURE 1.—Genetic alterations in the TRiC complex affect arsenic susceptibility. (A) As(III)-sensitive heterozygous diploid YKOs identified by genome-wide mutant fitness profiling. Essential genes are colored in red and nonessential genes in black. The network diagram was created with Cytoscape 2.0 (SHANNON *et al.* 2003). (B) Sensitivity of the heterozygous diploid YKOs of all eight TRiC subunits to As(III) at 450 μM. An *ho/ho*Δ mutant phenotypically indistinguishable from a wild-type yeast served as the control strain. (C) An *ho*Δ mutant harboring a vector or a plasmid overexpressing a TRiC subunit as indicated was tested for growth on solid SC −Ura that either contained or lacked 1 mM As(III).

and *TUB4*) that are directly involved in microtubule biogenesis and function (Figure 1A and Table S1). We directly tested three other heterozygous YKOs (*CCT2*, *CCT3*, and *CCT6*) of TRiC that were missed in the initial array-based screen due to low microarray hybridization signal intensities and found that they were also more sensitive to As(III) than a control strain (Figure 1B). Yeast cells overexpressing one of the TRiC complex genes, *CCT1*, were also partially arsenic resistant on solid medium (Figure 1C). Such an effect was also observed in liquid culture. Under unperturbed conditions, the growth rates of *ho*Δ mutants carrying an empty vector and overexpressing *TCC1* in a liquid synthetic medium were at 113 min/division and 115 min/division, respectively. In the presence of 450 μM of As(III), their growth rates were 181 min/division and 137 min/division, respectively. These results together suggest that As(III) might inhibit TRiC complex function.

Synthetic lethality interactions were previously observed between *CCT1* partial loss-of-function alleles and deletion mutations of the GimC complex, which acts as a cochaperone in TRiC-mediated actin and tubulin folding (SIEGERS *et al.* 1999). Thus, if As(III) inhibits TRiC, GimC deletion mutants should be arsenic hypersensitive. To test this prediction and to further extend the study of cellular response to As(III), we systematically investigated genome-wide haploid YKOs for As(III) sensitivity using dSLAM, a barcode microarray-based method for detecting gene-compound and gene–gene interactions (PAN *et al.* 2004). Upon individual validation, we found that 191 haploid YKOs were sensitive to As(III) at 400 μM or lower (Figure 2A and Table S2). The nine most sensitive ones directly affected either As(III) efflux (*arr1*Δ and *arr3*Δ) or the GimC complex (*gim3*Δ, *gim4*Δ, *gim5*Δ, *pac10*Δ, *pfd1*Δ, *yke2*Δ, and *yml094c-a*Δ, which deletes part of *GIM5*) (data not shown) and all GimC mutants were more sensitive than the ARR mutants when tested at 40 μM As(III) (Figure 2B and data not shown), further supporting the model that arsenic inhibits TRiC.

Most other As(III)-sensitive mutants were susceptible only to relatively high concentrations (Table S2). These included additional mutants affecting actin and microtubule biogenesis and those affecting peroxisome biogenesis, mitotic chromosome segregation, cell cycle

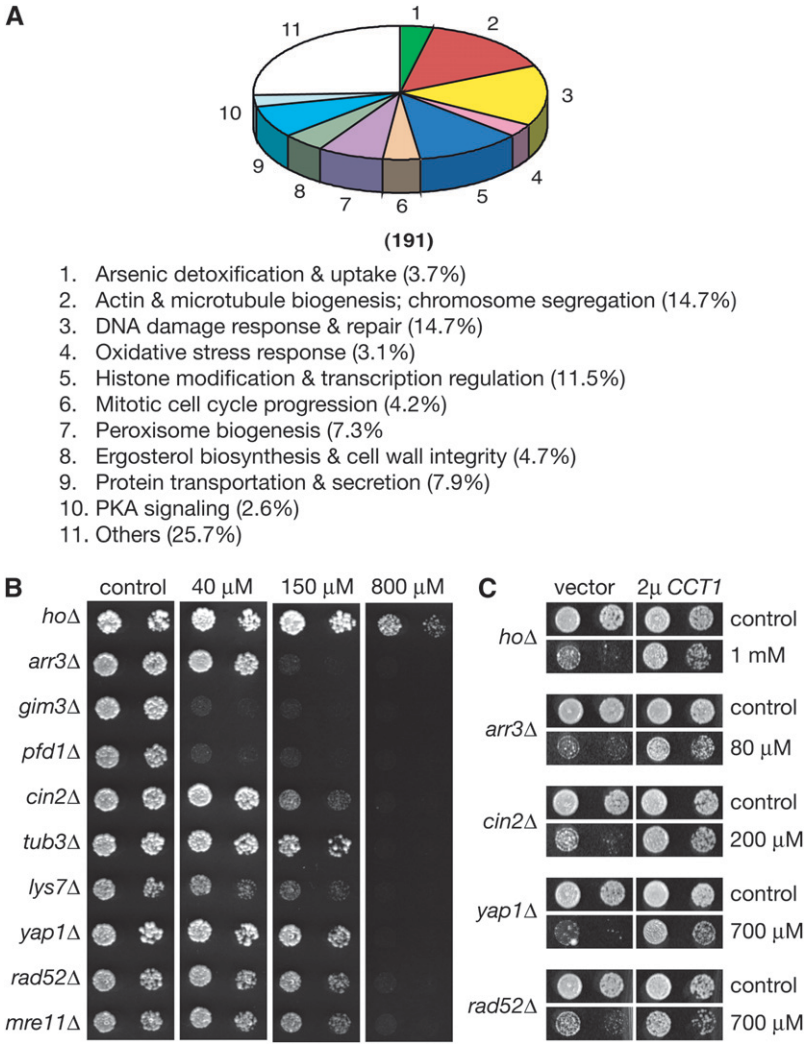

Figure 2.—Arsenic-sensitive haploid YKOs and their genetic relationships with *CCT1*. (A) As(III)-sensitive haploid deletion mutants identified by genome-wide mutant fitness profiling. A total of 191 were individually verified to be sensitive to As(III) at 400 μM. The number of mutants in each biological process affected and the corresponding percentage among all mutations identified were listed. This plot was derived from Table S2. (B) Growth of representative arsenic-sensitive haploid YKOs of indicated genotypes on a solid synthetic complete (SC) medium that either lacked or contained As(III) at 40 μM, 150 μM, and 800 μM. (C) Partial suppression of the arsenic sensitivity by *CCT1* overexpression in various mutants.

progression, histone modification, ergosterol biosynthesis, oxidative stress response, DNA repair, and others (Figure 2A and Table S2), consistent with results of recently performed screens using the haploid or homozygous diploid knockout mutants (Dilda *et al.* 2008; Jin *et al.* 2008; Thorsen *et al.* 2009). That mutants defective in oxidative stress response and DNA repair were sensitive to As(III) also agrees with a previous finding that As(III) stimulates the production of ROS (Tapio and Grosche 2006), which damage DNA molecules. The arsenic-sensitive phenotypes of some of these other mutants are likely related to TRiC inhibition because *CCT1* overexpression partially suppressed arsenic sensitivity in various mutants, including those of oxidative stress response and DNA repair (Figure 2C). Some of the affected pathways are likely required for buffering the effects of arsenic inhibition of TRiC. Others might well reflect additional independent *bona fide* arsenic targets in yeast.

Slowed protein synthesis confers As(III) resistance: We also identified 109 arsenic-resistant haploid YKOs and about 62.4% of them affected either ribosomal protein genes or those involved in ribosomal biogenesis (Figure 3A and Table S3). A similar connection between mutations in ribosomal biogenesis and arsenic resistance was also recently observed by others (Dilda *et al.* 2008). Although ribosomal proteins are essential, some are encoded by duplicated genes in yeast and deleting one copy is nonlethal. Interestingly, arsenic resistance of the ribosomal protein mutants largely correlated with their fitness defects under normal conditions (data not shown). We suspected that these mutants might have compromised capacity in protein synthesis, which leads to As(III) resistance. To test this hypothesis, we investigated the effects of inhibiting protein synthesis with a sublethal concentration of cycloheximide. Similar to the *rpl19b*Δ and *rps23b*Δ mutations that affect ribosomal protein genes, treatment with cycloheximide conferred yeast cells resistance to As(III) (Figure 3B). This relationship between protein synthesis and arsenic cytotoxicity is consistent with the model that As(III) inhibits TRiC, which facilitates the folding of newly synthesized polypeptides and their subsequent assembly into oligomeric complexes (Spiess *et al.* 2004).

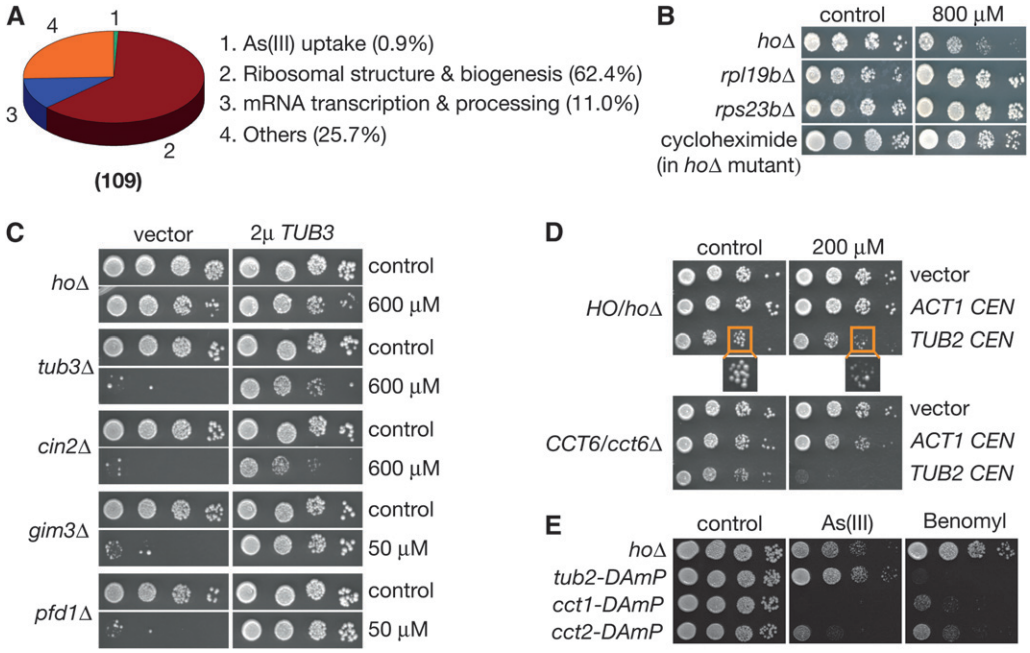

FIGURE 3.—The rate of protein synthesis and free β-tubulin modulate yeast arsenic sensitivity. (A) The distribution of arsenic-resistant haploid YKOs according to biological processes affected. This plot was derived from Table S3. (B) Cells of indicated genotypes were grown in an SC medium that either contained or lacked 800 μM of As(III). Cycloheximide was used at 10 ng/ml. (C) One of the α-tubulin genes *TUB3* was overexpressed from a 2μ plasmid in mutants defective in microtubule biogenesis. Cells were grown on solid SC −Ura either in the presence or absence of As(III). As(III) concentration used was 600 μM for the *ho*Δ, *tub3*Δ, and *cin2*Δ mutants and 50 μM for the *gim3*Δ and *pfd1*Δ mutants. (D) The β-tubulin gene *TUB2* and the actin gene *ACT1* were expressed in mutants of indicated genotypes from a centromere-based plasmid. Cells were grown on solid SC that lacked uracil (SC −Ura) either in the presence or absence of 200 μM of As(III). (E) Strains of indicated genotypes were grown on solid YPD with or without As(III) (1 mM) or benomyl (20 μg/ml).

Inhibition of TRiC by As(III) likely has two distinct types of effects: (1) production of insufficient quantities of correctly folded substrates and assembled complexes that are essential for viability and (2) accumulation of incorrectly folded substrates or unassembled subunits that are toxic.

β-Tubulin contributes to As(III) toxicity: One such TRiC substrate is β-tubulin, which causes growth defects in yeast cells when overexpressed and not dimerized with α-tubulin (ARCHER *et al.* 1995). Presumably, β-tubulin polypeptides produced at lower rates (resulting from slowed protein translation) in ribosomal protein mutants or cycloheximide-treated cells were more compatible with the capacity of arsenic-crippled TRiC complex. As a result, unfolded polypeptides and/or unassembled toxic free β-tubulin molecules might have been accumulated at lower levels, mitigating As(III) toxicity. To test this hypothesis, we investigated whether β-tubulin contributes to As(III) toxicity by genetically perturbing the relative ratio between α- and β-tubulins. We first modestly overexpressed *TUB2* (the β-tubulin gene) from a centromeric plasmid under control of its endogenous promoter and tested its effects on the growth and arsenic sensitivity of *HO/ho*Δ (a surrogate wild type) and *CCT6/cct6*Δ heterozygous diploid mutants. Modest overexpression of *TUB2* made the *HO/ho*Δ mutant slightly yet reproducibly more sensitive to As(III) (Figure 3D). It also noticeably hampered growth of the *CCT6/cct6*Δ mutant in the absence of As(III) and even more so in its presence (Figure 3D). In comparison, modest overexpression of *ACT1*, which encodes another important cytoskeletal substrate of TRiC, actin, had no effect (Figure 3C). In agreement with these results, deleting *TUB3*, a nonessential gene encoding α-tubulin, caused As(III) hypersensitivity (Figures 2B and 3C). Overexpression of *TUB3* from a high copy plasmid also suppressed As(III) toxicity in *cin2*Δ, *gim3*Δ, and *pfd1*Δ mutants (Figure 3C), which are defective in tubulin folding and dimerization. Similar results were observed when *TUB1*, an essential α-tubulin gene highly homologous to *TUB3*, was overexpressed (data not shown). In these mutants, overexpression of α-tubulin likely allowed more efficient folding and/or incorporation of β-tubulin molecules into nontoxic heterodimers due to the increased abundance of available α-tubulin molecules. These results together indicated that yeast cells with a relatively high β/α-tubulin ratio are sensitized to As(III) and those with a low β/α-tubulin ratio are more resistant to the drug. Thus unfolded and/or folded yet free β-tubulin molecules apparently contribute to As(III) cytotoxicity.

Arsenic unlikely directly inhibits microtubule function in yeast: It has been proposed that As(III) directly binds to tubulins and disrupts their functions in mammalian cells (LI and BROOME 1999). In particular, As(III) was shown to directly bind to β-tubulin isolated from a human breast cancer cell line and structural modeling suggested the amino acid residue Cys12 is key to such a physical interaction (ZHANG *et al.* 2007). This model of arsenic action would be consistent with most of

the genetic evidence described above. However, it is not consistent with other genetic evidence. We found that a *tub2–DAmP* mutant (Breslow *et al.* 2008), which presumably expresses *TUB2* at a lower level as compare to a wild type due to mRNA instability, responds to As(III) and the well-known microtubule poison benomyl very differently. Consistent with the idea that benomyl directly binds to and inihibits microtubules, the *tub2–DAmP* was hypersensitive to this drug (Figure 3E). The latter result also implies that *TUB2* expression is indeed reduced in the DAmP allele. In contrast to the hypothesis that As(III) directly affects microtubules, the *tub2–DAmP* strain was slightly more resistant to As(III) than the wild type (Figure 3E), a highly reproducible phenotype. A *TUB2/tub2*Δ heterozygous diploid mutant was similarly hypersensitive to benomyl but slightly more resistant to As(III) as compared to a *HO/ho*Δ control strain (data not shown). In contrast to the *tub2–DAmP* mutant, both the *cct1–DAmP* and *cct2–DAmP* mutants were hypersensitive to both As(III) and benomyl. These results suggest that As(III) unlikely inhibit yeast growth by binding to microbutules as benomyl does. Of course, it is still possible that arsenic binds to yeast microtubules but has a different effect than benomyl. However, the Cys12 residue critical for arsenic binding to human β-tubulin is not conserved in its yeast ortholog. The genetic results are also more consistent with the model that As(III) inhibits the TRiC complex, which is required to compensate for the loss of microtubule functions in the presence of benomyl due to its essential functions in microtubule biogenesis (Ursic *et al.* 1994; Siegers *et al.* 2003).

Arsenic affects TRiC function *in vivo*: Defects in TRiC were previously shown to distort morphological organization of both actin and microtubule filaments (Ursic *et al.* 1994; Siegers *et al.* 2003). If As(III) inhibits TRiC, we expected that arsenic treatment of wild-type yeast cells would have similar effects, and this was exactly what we observed. Actin filaments are typically polarized to emerging buds under normal conditions (Figure 4A) (Adams and Pringle 1984; Kilmartin and Adams 1984). In the presence of As(III), such polarization disappeared (Figure 4A). Arsenic treatment also distorted the mitotic microtubule structures (Figure 4A). Similar observations were recently made in another study (Jin *et al.* 2008), although the exact microtubule morphology change caused by arsenic treatment shown there was different from what we saw. Such difference was likely caused by different experimental protocols. In this other study, the intrinsic fluorescence of GFP tagged α-tubulin was observed, whereas we used immunostaining. Despite this, the fact that arsenic treatment affects the morphology of both actin and microtubule filaments strongly support the model that As(III) inhibits TRiC functions *in vivo*.

We next investigated whether As(III) might interfere with the physical interaction between TRiC and its substrates. In addition to the major substrates actin and tubulins, TRiC is required for folding of cytoplasmic proteins such as Cdc55p in yeast (Siegers *et al.* 2003). We found that As(III) reproducibly and significantly reduced physical interaction between TRiC and Cdc55p in coimmunoprecipitation assays (Figure 4B), further indicating that As(III) directly affects TRiC functions. However, arsenic had no effect on the physical interaction between TRiC and β-tubulin (data not shown) and its effect on the interaction between TRiC and actin was inconclusive. Out of three independent coimmunoprecipitation experiments, we found that As(III) partially reduced TRiC binding to actin in one experiment and did not see any effect in the other two (data not shown). Thus, As(III) inhibits TRiC binding to some substrates (*i.e.*, Cdc55p) but not to others *in vivo* (β-tubulin).

Arsenic inhibits TRiC activity *in vitro*: Eukaryotic pyruvate dehydrogenase (PDH), which consumes pyruvate to form acetyl-CoA while reducing NAD^+ to NADH, has long been considered a primary target for arsenic (Schiller *et al.* 1977). A possible consequence of arsenic inhibition of PDH is disruption of energy production and lowered intracellular ATP/ADP ratio. TRiC folding of substrates absolutely requires ATP hydrolysis (Spiess *et al.* 2004) and As(III) might inhibit TRiC function indirectly by inactivating PDH and thereby damping intracellular ATP concentration. However, we consider this unlikely because PDH is nonessential in yeast. In addition, we did not observe a synthetic lethality or slow growth interaction between a PDH (*pda1*Δ) mutation and a GimC mutation (*pfd1*Δ) (data not shown).

We next tested the possibility that As(III) directly inactivates TRiC using a well-characterized *in vitro* assay that monitors the ability of purified chaperonin to fold chemically denatured ^{35}S-actin (Meyer *et al.* 2003). We found that addition of 1 mM As(III) to a folding reaction using purified bovine TRiC significantly inhibited actin folding. Such inhibition was observed both when the inhibitor was added before and shortly after substrate binding to TRiC. Here binding of TRiC to actin was not inhibited by As(III) (Figure 4C). Yet actin folding activity was still inhibited, suggesting that As(III) inactivates TRiC after substrate binding. Similarly, As(III) inhibited substrate folding by a TRiC-like archaeal complex, the Mm-Cpn chaperonin from *Methanococcus maripaludis*, which is ~40% identical to its human counterpart (Figure 4D). Together, these results support the idea that As(III) directly inhibits the folding activity of TRiC and TRiC-like chaperones.

We also found that inhibition of TRiC by arsenic *in vitro* was reversible because its activity was recovered after gel filtration (data not shown), ruling out direct covalent modification of TRiC by As(III) as a mechanism of action. Such reversibility was also observed with arsenic inhibition of yeast growth; nearly 100% of yeast cells regained colony formation capacity after being

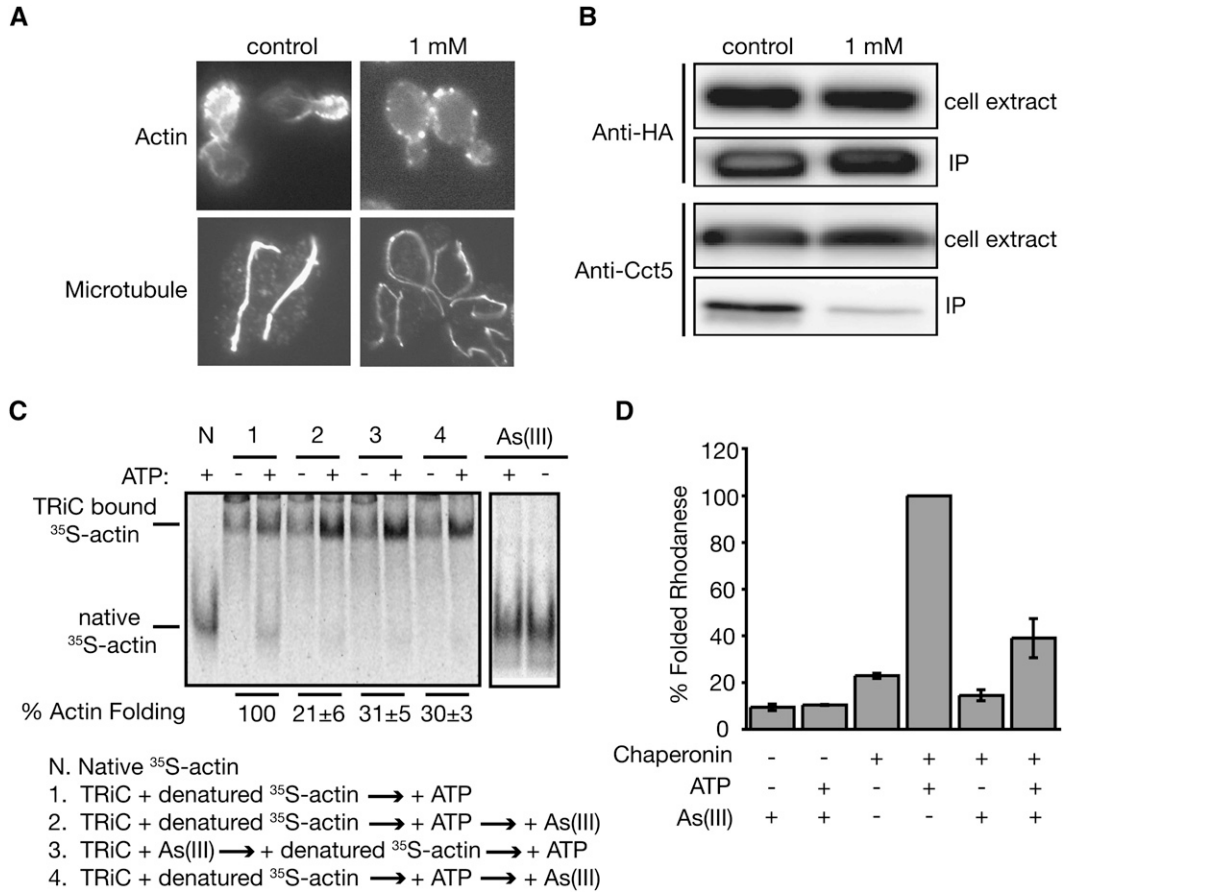

FIGURE 4.—As(III) inhibits TRiC functions. (A) Wild-type yeast (BY4743) cells were grown in liquid YPD either in the absence or presence of 1 mM of As(III) for 3 hr. Actin was stained with rhodamine-phalloidin and microtubules were visualized with an anti-α–tubulin antibody. (B) ATP-depleted cell lysates prepared from yeast cells expressing Cdc55–3HA grown in liquid YPD that either contained or lacked 1 mM As(III) were subjected to immunoprecipitation with anti-HA antibody. Western blots of the total cell extracts (5μg) and the immunoprecipitates (IP) from lysates containing 200 μg total protein were analyzed with an anti-HA antibody and an antibody against one of the TRiC subunits Cct5. (C) *In vitro* binding and folding of denatured [^{35}S]-actin by bovine TRiC both in the presence and absence of 1 mM As(III) were assessed by native gel analysis followed by autoradiography. Three (2, 3, and 4) different schemes of arsenic treatment were tested. Native [^{35}S]-actin samples incubated with or without As(III) were included as controls (right two lanes). The extent of As(III) inhibition in each condition was quantified for three independent experiments and expressed as percentage of actin folding relative to the untreated control. (D) *In vitro* rhodanese folding by the *M. maripaludis* TRiC-like chaperonin (Mm-Cpn) was assessed in the presence and absence of 1 mM sodium arsenite as described (KUSMIERCZYK and MARTIN 2003).

incubated in the presence of inhibitory concentration of the drug (>2 mM) for over 24 hr at 30° (data not shown).

Detoxification mutations sensitize TRiC defective cells toward As(III): Arsenic concentrations required for inhibiting growth of wild-type yeast cells are much higher than needed for arsenic chemotherapy and toxicity in human cells. To mitigate such difference, we next investigated whether arsenic inhibition of TRiC at clinically achievable doses could inhibit growth of relatively healthy yeast cells. To do this, we first performed a genome-wide synthetic As(III)-hypersensitivity screen to identify secondary mutations that further sensitize a *pfd1*Δ mutant, which does not have obvious growth defect on its own but does exhibit partial defect in TRiC-mediated actin and tubulin folding (GEISER *et al.* 1997; VAINBERG *et al.* 1998), to 5 μM of As(III) (Figure 5A). We identified and individually confirmed a large number of such mutations (Table S4). Among them, both *arr1*Δ and *arr3*Δ rendered the *pfd1*Δ mutant highly sensitive to 5 μM of As(III) without affecting its growth rate under normal conditions (Figure 5B and Table S4). Growth of the *arr1*Δ *pfd1*Δ and *arr3*Δ *pfd1*Δ double mutants was also significantly inhibited by a lower concentration of arsenic (2 μM) (Figure 5B). Thus, at clinically effective doses, arsenic inactivation of TRiC indeed significantly inhibited the growth of otherwise healthy yeast cells. These results indicate that, at the mechanistic level, arsenic modes of actions may well be the same in both yeast and human, even though the wild-type yeast cells seem to be more resistant to As(III) than human cells. Interestingly, Arr1p is a transcription factor required for

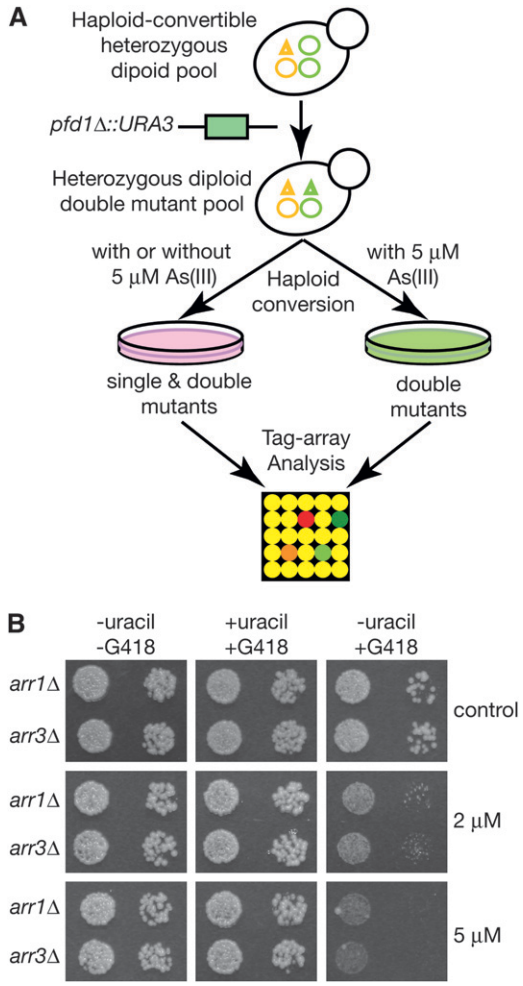

Figure 5.—A genome-wide screen identifies double mutants hypersensitive to low concentrations of arsenic. (A) A high-efficiency *pfd1Δ::URA3* gene disruption cassette was transformed into a pool of haploid-convertible heterozygous diploid yeast knockout mutants. After sporulation, a pool of haploid double knockout mutants were derived from the heterozygous diploid double mutant pool in the presence of 5 μM of As(III). A separate pool of haploid single and double mutants were also similarly derived either in the presence or absence of 5 μM of As(III). Relative representation of each knockout mutation in both pools was compared by TAG-array analysis (Pan *et al.* 2004). (B) Haploid-convertible *ARR1/arr1Δ::kanMX PFD1/pfd1Δ::URA3* and *ARR3/arr3Δ::kanMX PFD1/pfd1Δ::URA3* diploid double mutants were sporulated and spotted on a haploid selection medium that either lacked both uracil and G418 (to select for Ura^+ single and double mutants), contained both uracil and G418 (to select for G418-resistant single and double mutants), or lacked uracil but contained G418 (to select for the double mutants). Cell growth under each condition was assessed both in the absence (control) and presence of 2 μM or 5 μM of As(III) and photographed.

expression of Arr3p, an arsenite transporter that actively pumps the drug out of yeast cells (Ghosh *et al.* 1999). Mammalian genomes do not seem to encode an Arr3p-like arsenic transporter, the absence of which might allow for more effective accumulation of intracellular As(III).

DISCUSSION

By using a combination of functional genomic, genetic, and biochemical studies, we have investigated the genetic determinants of arsenic susceptibility in yeast and elucidated a mechanism of action by arsenic common to both eukaryotes and archaea. Our data suggest that arsenic inhibits the function(s) of the chaperonin complex. Similar functional genomic studies have been recently reported (Dilda *et al.* 2008; Jin *et al.* 2008; Thorsen *et al.* 2009). Although there was considerable overlap among all of these studies regarding the lists of arsenic-sensitive and -resistant mutants identified, our study is distinctly different from these others, which studied only the haploid and/or homozygous diploid knockout mutant libraries that lack mutants of essential genes. In contrast, we first studied the genome-wide heterozygous diploid mutants, which directly and dramatically revealed the essential TRiC complex as a candidate target of As(III) via drug-induced haploinsufficiency. We subsequently corroborated this finding by identifying As(III)-hypersensitive and -resistant haploid mutants. In particular, we have put an emphasis on the most sensitive haploid knockout mutant(s) with the premise that it likely affects functions most closely related to the arsenic target(s). That all 6 mutants of the GimC complex exhibited the highest sensitivity toward low concentrations of As(III) (Figure 2B and Table S2) further supported the idea that TRiC is the target. More importantly, we provided further evidence that As(III) inhibits TRiC functions both *in vivo* and *in vitro*. Such a conclusion is also consistent with a previous observation made in mouse Swiss 3T3 cells that treatment with 30 μM of arsenic leads to distorted organization of both actin and microtubule filaments (Li and Chou 1992). Lastly, with subtle modification of the previously described dSLAM methodology (Pan *et al.* 2004), we also demonstrated that it is possible to systematically identify genome-wide double mutations that confer hypersensitivity to a given drug in a high throughput manner. This will allow for expansion in the elucidation of genetic interaction networks involved in drug response to beyond monogenic traits.

Despite that As(III) concentrations used in most of our experiments were relatively high, our results are likely relevant to arsenic effects on human health. First, our results with the apparently healthy *arr1Δ pfd1Δ* and *arr3Δ pfd1Δ* double mutants (Figure 5B) have demonstrated that low concentrations of arsenic can inhibit cell growth in yeast. That human cells are more susceptible might also be due to stress-induced apoptosis that is basically lacking in yeast cells. Second, both yeast and human cells accumulate high levels of arsenic after exposure to low concentrations and this is more obvious in human cells than in yeast. It was shown that $\sim 10^6$ wild-type yeast cells exposed to 160 μM of arsenic for 2 hr accumulate ~0.163 nmol of the drug (Dilda

et al. 2008), equivalent to a final intracellular concentration of ~2.3 mM, assuming an average volume of a haploid yeast cell of ~70 fl (Sherman 2002). Similarly, ~10^6 human APL cells (NB4) exposed to 20 μM of arsenic for 4 hr accumulated ~0.73 nmol of the drug (Dilda *et al.* 2008), equivalent to an intracellular concentration of ~0.7 mM, assuming an average volume of of ~1040 fl for an NB4 cell (Miossec-Bartoli *et al.* 1999). As(III) concentrations within cells of certain human organs and tissues or within some intracellular compartments might be even higher. Thus our observation of TRiC inhibition by 1 mM of As(III) *in vitro* could be relevant *in vivo* even when mammalian cells are exposed to relatively low levels of As(III). Third, our *in vitro* assays might have underdetected the potency of arsenic inhibition of TRiC. In the protein-folding assays, we had to include 1 mM of DTT, which is absolutely required for substrate folding by TRiC and Mm-Cpn (J. Frydman, unpublished observations). The presence of DTT in the folding assays likely at least partially reversed the inhibitory effects of arsenic on TRiC and Mm-Cpn. Unfortunately, we could not test the effects of lower concentrations of As(III) on TRiC activities due to this technical limitation of the assay.

Among the heavy metals that interact with thiol groups, As(III) inhibition of TRiC seems to be specific. One piece of supporting evidence is that mutants of the prefoldin complexes, which are hypersensitive to As(III), did not exhibit sensitivity toward Cd^{2+} when compared to a wild-type strain (data not shown). However, currently it is not clear how As(III) inhibits the TRiC complex at the biochemical level. It did not seem to inhibit TRiC's substrate binding (Figure 4C) or its ATPase activity. In fact, arsenic stimulated the ATPase activity of TRiC by approximately twofold (data not shown). Given the similar inhibitory effects observed when As(III) was added both before and shortly after substrate binding (Figure 4C), it is possible that it blocks a late step of the process, for example, release of correctly folded products from the chaperonin complex. This might gradually lead to accumulation of unproductive TRiC complex and reduction in its overall productivity. This might partly explain why arsenic reproducibly inhibits TRiC binding to Cdc55 but not actin and tubulin. Possibly, most TRiC molecules within arsenic-treated cells are stuck with the more abundant substrates such as actin and tubulin.

That TRiC is required for folding and maturation of as much as ~9–15% of all cytosolic proteins in mammals (Thulasiraman *et al.* 1999) might also at least partly explain the pleiotropic effects of arsenic on human health. For example, exposure to arsenic has been linked to cancers and neuropathy. The former might be related to the fact that TRiC is required for the assembly of the Von Hippel-Lindau (VHL) tumor suppressor complex (Feldman *et al.* 1999), which plays a positive role in stabilizing and activating p53 (Roe *et al.* 2006), a major tumor suppressor commonly mutated in various human cancers. Arsenic inhibition of TRiC might thus indirectly downregulate p53 activity and cause cancers, a model consistent with the observation that arsenic inhibits p53 activation in response to DNA damage (Tang *et al.* 2006). In addition, mutating TRiC subunit genes *CCT5* and *CCT4* are directly implicated in sensory neuropathy in both human patients and in a rat model (Lee *et al.* 2003; Bouhouche *et al.* 2006).

We thank Katja Siegers for providing the anti-Cct5p antibody and a yeast strain that expresses Cdc55p–3HA (Siegers *et al.* 2003). We are also grateful to David Drubin and Andy Hoyt for anti-α–tubulin antibodies and Pamela Meluh for an anti-β–tubulin antibody. We thank Robert Cohen and Pamela Meluh for helpful comments on the manuscript. This work was supported in part by National Institutes of Health (NIH) grants HG02432 and RR020839 to J.D.B, by NIH grant HG004840 to X.P., by NIH grant RR019409 to J.M.M., and by NIH grant GM74074 and a grant from the NIH Roadmap Initiative on Nanomedicine to J.F.

LITERATURE CITED

Adams, A. E., and J. R. Pringle, 1984 Relationship of actin and tubulin distribution to bud growth in wild-type and morphogenetic–mutant Saccharomyces cerevisiae. J. Cell Biol. **98:** 934–945.

Archer, J. E., L. R. Vega and F. Solomon, 1995 Rbl2p, a yeast protein that binds to beta-tubulin and participates in microtubule function in vivo. Cell **82:** 425–434.

Bouhouche, A., A. Benomar, N. Bouslam, T. Chkili and M. Yahyaoui, 2006 Mutation in the epsilon subunit of the cytosolic chaperonin-containing t-complex peptide-1 (Cct5) gene causes autosomal recessive mutilating sensory neuropathy with spastic paraplegia. J. Med. Genet. **43:** 441–443.

Breslow, D. K., D. M. Cameron, S. R. Collins, M. Schuldiner, J. Stewart-Ornstein *et al.*, 2008 A comprehensive strategy enabling high-resolution functional analysis of the yeast genome. Nat. Methods **5:** 711–718.

Bukau, B., and A. L. Horwich, 1998 The Hsp70 and Hsp60 chaperone machines. Cell **92:** 351–366.

Dilda, P. J., G. G. Perrone, A. Philp, R. B. Lock, I. W. Dawes *et al.*, 2008 Insight into the selectivity of arsenic trioxide for acute promyelocytic leukemia cells by characterizing Saccharomyces cerevisiae deletion strains that are sensitive or resistant to the metalloid. Int. J. Biochem. Cell Biol. **40:** 1016–1029.

Feldman, D. E., V. Thulasiraman, R. G. Ferreyra and J. Frydman, 1999 Formation of the VHL-elongin BC tumor suppressor complex is mediated by the chaperonin TRiC. Mol. Cell **4:** 1051–1061.

Frydman, J., and F. U. Hartl, 1996 Principles of chaperone-assisted protein folding: differences between in vitro and in vivo mechanisms. Science **272:** 1497–1502.

Geiser, J. R., E. J. Schott, T. J. Kingsbury, N. B. Cole, L. J. Totis *et al.*, 1997 Saccharomyces cerevisiae genes required in the absence of the CIN8-encoded spindle motor act in functionally diverse mitotic pathways. Mol. Biol. Cell **8:** 1035–1050.

Ghosh, M., J. Shen and B. P. Rosen, 1999 Pathways of As(III) detoxification in Saccharomyces cerevisiae. Proc. Natl. Acad. Sci. USA **96:** 5001–5006.

Giaever, G., D. D. Shoemaker, T. W. Jones, H. Liang, E. A. Winzeler *et al.*, 1999 Genomic profiling of drug sensitivities via induced haploinsufficiency. Nat. Genet. **21:** 278–283.

Gietz, R. D., and A. Sugino, 1988 New yeast-Escherichia coli shuttle vectors constructed with in vitro mutagenized yeast genes lacking six-base pair restriction sites. Gene **74:** 527–534.

Gutsche, I., L. O. Essen and W. Baumeister, 1999 Group II chaperonins: new TRiC(k)s and turns of a protein folding machine. J. Mol. Biol. **293:** 295–312.

Jin, Y. H., P. E. Dunlap, S. J. McBride, H. Al-Refai, P. R. Bushel *et al.*, 2008 Global transcriptome and deletome profiles of yeast exposed to transition metals. PLoS Genet. **4:** e1000053.

Kilmartin, J. V., and A. E. Adams, 1984 Structural rearrangements of tubulin and actin during the cell cycle of the yeast Saccharomyces. J. Cell Biol. **98:** 922–933.

Kusmierczyk, A. R., and J. Martin, 2003 Nucleotide-dependent protein folding in the type II chaperonin from the mesophilic archaeon Methanococcus maripaludis. Biochem. J. **371:** 669–673.

Lee, M. J., D. A. Stephenson, M. J. Groves, M. G. Sweeney, M. B. Davis *et al.*, 2003 Hereditary sensory neuropathy is caused by a mutation in the delta subunit of the cytosolic chaperonin-containing t-complex peptide-1 (Cct4) gene. Hum. Mol. Genet. **12:** 1917–1925.

Li, W., and I. N. Chou, 1992 Effects of sodium arsenite on the cytoskeleton and cellular glutathione levels in cultured cells. Toxicol. Appl. Pharmacol. **114:** 132–139.

Li, Y. M., and J. D. Broome, 1999 Arsenic targets tubulins to induce apoptosis in myeloid leukemia cells. Cancer Res. **59:** 776–780.

Lum, P. Y., C. D. Armour, S. B. Stepaniants, G. Cavet, M. K. Wolf *et al.*, 2004 Discovering modes of action for therapeutic compounds using a genome-wide screen of yeast heterozygotes. Cell **116:** 121–137.

Meyer, A. S., J. R. Gillespie, D. Walther, I. S. Millet, S. Doniach *et al.*, 2003 Closing the folding chamber of the eukaryotic chaperonin requires the transition state of ATP hydrolysis. Cell **113:** 369–381.

Miller, Jr., W. H., H. M. Schipper, J. S. Lee, J. Singer and S. Waxman, 2002 Mechanisms of action of arsenic trioxide. Cancer Res. **62:** 3893–3903.

Miossec-Bartoli, C., L. Pilatre, P. Peyron, E. N. N'Diaye, V. Collart-Dutilleul *et al.*, 1999 The new ketolide HMR3647 accumulates in the azurophil granules of human polymorphonuclear cells. Antimicrob. Agents Chemother. **43:** 2457–2462.

Nordstrom, D. K., 2002 Public health. Worldwide occurrences of arsenic in ground water. Science **296:** 2143–2145.

Pan, X., and J. Heitman, 2002 Protein kinase A operates a molecular switch that governs yeast pseudohyphal differentiation. Mol. Cell. Biol. **22:** 3981–3993.

Pan, X., D. S. Yuan, D. Xiang, X. Wang, S. Sookhai-Mahadeo *et al.*, 2004 A robust toolkit for functional profiling of the yeast genome. Mol. Cell **16:** 487–496.

Ramirez, P., D. A. Eastmond, J. P. Laclette and P. Ostrosky-Wegman, 1997 Disruption of microtubule assembly and spindle formation as a mechanism for the induction of aneuploid cells by sodium arsenite and vanadium pentoxide. Mutat. Res. **386:** 291–298.

Rieder, S. E., L. M. Banta, K. Kohrer, J. M. McCaffery and S. D. Emr, 1996 Multilamellar endosome-like compartment accumulates in the yeast vps28 vacuolar protein sorting mutant. Mol. Biol. Cell **7:** 985–999.

Roe, J. S., H. Kim, S. M. Lee, S. T. Kim, E. J. Cho *et al.*, 2006 p53 stabilization and transactivation by a von Hippel-Lindau protein. Mol. Cell **22:** 395–405.

Schiller, C. M., B. A. Fowler and J. S. Woods, 1977 Effects of arsenic on pyruvate dehydrogenase activation. Environ. Health Perspect. **19:** 205–207.

Shannon, P., A. Markiel, O. Ozier, N. S. Baliga, J. T. Wang *et al.*, 2003 Cytoscape: a software environment for integrated models of biomolecular interaction networks. Genome Res. **13:** 2498–2504.

Sherman, F., 2002 Getting started with yeast. Methods Enzymol. **350:** 3–41.

Siegers, K., T. Waldmann, M. R. Leroux, K. Grein, A. Shevchenko *et al.*, 1999 Compartmentation of protein folding in vivo: sequestration of non-native polypeptide by the chaperonin-GimC system. EMBO J. **18:** 75–84.

Siegers, K., B. Bolter, J. P. Schwarz, U. M. Bottcher, S. Guha *et al.*, 2003 TRiC/CCT cooperates with different upstream chaperones in the folding of distinct protein classes. EMBO J. **22:** 5230–5240.

Spiess, C., A. S. Meyer, S. Reissmann and J. Frydman, 2004 Mechanism of the eukaryotic chaperonin: protein folding in the chamber of secrets. Trends Cell. Biol. **14:** 598–604.

Tang, F., G. Liu, Z. He, W. Y. Ma, A. M. Bode *et al.*, 2006 Arsenite inhibits p53 phosphorylation, DNA binding activity, and p53 target gene p21 expression in mouse epidermal JB6 cells. Mol. Carcinog. **45:** 861–870.

Tapio, S., and B. Grosche, 2006 Arsenic in the aetiology of cancer. Mutat. Res. **612:** 215–246.

Thorsen, M., G. G. Perrone, E. Kristiansson, M. Traini, T. Ye *et al.*, 2009 Genetic basis of arsenite and cadmium tolerance in Saccharomyces cerevisiae. BMC Genomics **10:** 105.

Thulasiraman, V., C. F. Yang and J. Frydman, 1999 In vivo newly translated polypeptides are sequestered in a protected folding environment. EMBO J. **18:** 85–95.

Tseng, C. H., 2004 The potential biological mechanisms of arsenic-induced diabetes mellitus. Toxicol. Appl. Pharmacol. **197:** 67–83.

Ursic, D., J. C. Sedbrook, K. L. Himmel and M. R. Culbertson, 1994 The essential yeast Tcp1 protein affects actin and microtubules. Mol. Biol. Cell **5:** 1065–1080.

Vainberg, I. E., S. A. Lewis, H. Rommelaere, C. Ampe, J. Vandekerckhove *et al.*, 1998 Prefoldin, a chaperone that delivers unfolded proteins to cytosolic chaperonin. Cell **93:** 863–873.

Weber, F., and M. Hayer-Hartl, 2000 Refolding of bovine mitochondrial rhodanese by chaperonins GroEL and GroES. Methods Mol. Biol. **140:** 117–126.

Zhang, X., F. Yang, J. Y. Shim, K. L. Kirk, D. E. Anderson *et al.*, 2007 Identification of arsenic-binding proteins in human breast cancer cells. Cancer Lett. **255:** 95–106.

Communicating editor: M. D. Rose

GENETICS

Supporting Information
http://www.genetics.org/cgi/content/full/genetics.110.117655/DC1

Trivalent Arsenic Inhibits the Functions of Chaperonin Complex

Xuewen Pan, Stefanie Reissman, Nick R. Douglas, Zhiwei Huang, Daniel S. Yuan, Xiaoling Wang, J. Michael McCaffery, Judith Frydman and Jef D. Boeke

DOI: 10.1534/genetics.110.117655

FILE S1

Supporting Methods

Genome-wide haplo-insufficiency screen As_2O_3 (Sigma-Aldrich, St. Louis, MO) was first dissolved in NaOH as a 400 mM stock solution of sodium arsenite. A pool of 5996 haploid-convertible heterozygote diploid YKOs was constructed as previously described (PAN *et al.* 2004). ~2 x 10^6 cells of this pool were directly inoculated into 100 ml of YPD liquid that contains (experiment) or lacks (control) 450 mM of sodium arsenite and incubated by shaking at 30 °C for 10 generations. After this outgrowth, cells were harvested from both the control and experimental samples for genomic DNA preparation and TAG array analysis of relative representation of each YKO in both pools as described (PAN *et al.* 2004). YKOs with control/experiment hybridization ratios ≥ 2.0 were selected as candidate drug sensitive mutant for individual validation.

Screens for arsenic-hypersensitive and -resistant haploid YKOs The screens were done essentially as described in Pan et al. (PAN *et al.* 2004). Briefly, the haploid-convertible heterozygote dipoid YKO pool was sporulated and pools of isogenic *MAT***a** haploid cells were derived by growth on a haploid selection (SC-Leu-His-Arg+canavanine+G418 with glutamic acid instead of ammonium sulfate as the nitrogen source) that either contained (experiment) or lacked (control) sodium arsenite. Relative representation of each YKO in drug-treated and untreated pools was compared by TAG-array analysis. The concentrations of sodium arsenite used were 100 mM, 200 mM, 400 mM, 800 mM, and 1600 mM. Experiments with the lower concentrations identified As(III)-sensitive mutants, whereas the highest concentration (1600 mM) revealed As(III)-resistant mutants, which should be over-represented in the drug-treated population because growth of most other haploid YKOs is significantly inhibited.

Synthetic arsenic-hypersensitivity screen This screen was carried out essentially like a typical dSLAM screen (PAN *et al.* 2004) with the following modifications. A *pfd1*Δ*::URA3* construct that contains ~1.5 kb flanking targeting sequences was PCR amplified with a pair of primers (5' GCTGTATCGCACTCAAACAA 3' and 5' TACACTACTACACCTCTGCAT 3') and *en masse* transformed into a pool of haploid convertible heterozygote diploid YKOs. The resultant heterozygous diploid double mutant pool was sporulated and a *MAT***a** haploid double mutant (*pfd1*Δ*::URA3 xxx*Δ*::kanMX*, "*xxx*Δ" stands for any yeast gene deletion) pool was derived by selection on a haploid selection medium that lacked uracil but contained 5 mM of sodium arsenite (SC-Leu-His-Arg-Ura+canavanine+G418+ arsenite). As a control, a mixed population of *MAT***a** haploid single (*xxx*Δ*::kanMX*) and double (*pfd1*Δ*::URA3 xxx*Δ*::kanMX*) mutants was selected on a haploid selection medium that contained uracil but lacked arsenic (SC-Leu-His-Arg+canavanine+G418). Relative representation of each YKO in these two populations was compared by TAG-array analysis. This screen identified mutations that cause growth defects in a *pfd1*Δ mutant both in the absence and

presence of arsenic 5 mM As(III). These were subsequently confirmed and distinguished by testing individual mutants both in the presence and absence of the drug as described below.

Individual confirmation of arsenic-hypersensitive and -resistant YKOs To confirm the arsenic-sensitive heterozygous diploid mutants identified by TAG-array, individual strains were spotted onto solid YPD plus G418 that either contained or lacked 450 mM of sodium arsenite and incubated at 30°C for 3 days. The results were reported in Fig. 1a and Supporting Table 1. To confirm arsenic-hypersensitive or -resistant haploid YKOs, individual haploid convertible heterozygous diploid mutants were sporulated, spotted onto haploid selection media that either contained or lacked sodium arsenite at indicated concentrations and incubated at 30°C for 3 days. The confirmed results were reported in Supporting Tables 2 and 3. To confirm mutations that cause growth defects in a *pfd1*Δ mutant or those that specifically sensitizes the *pfd1*Δ mutant to arsenic, individual haploid convertible heterozygote diploid mutants were transformed with a *pfd1*Δ*::URA3* construct to create diploid double mutants. Two independent transformants for each were tested by random spore analysis (RSA) (PAN *et al.* 2004). Haploid progeny were spotted as 10X serial dilutions on SC-Leu-His-Arg+canavanine+G418, which allows for growth of *xxx*Δ*::kanMX* and *pfd1*Δ*::URA3 xxx*Δ*::kanMX* cells, SC-Leu-His-Arg-Ura+canavanine, which allows for growth of *pfd1*Δ*::URA3* and *pfd1*Δ*::URA3 xxx*Δ*::kanMX* cells, and SC-Leu-His-Arg-Ura+canavanine+G418, which allows for growth of only the *pfd1*Δ*::URA3 xxx*Δ*::kanMX* double-mutant cells) and incubated at 30°C for 2 to 3 days. This was similarly carried out in the presence of 5 μM sodium arsenite. The confirmed results were reported in Supporting Table 4.

TABLE S1

Arsenic-hypersensitive heterozygous diploid YKOs

ORF Name	Gene name	Biological Process	Essential[a]
YDR212W	*CCT1*	protein folding	Y
YDL143W	*CCT4*	protein folding	Y
YJR064W	*CCT5*	protein folding	Y
YJL111W	*CCT7*	protein folding	Y
YJL009W	*YJL009W*[b]	Dubious ORF overlaps with *CCT8*, protein folding	Y
YAL038W	*CDC19*	Glycolysis	Y
YLR293C	*GSP1*	nuclear organization and biogenesis	Y
YMR296C	*LCB1*	sphingolipid biosynthesis	Y
YGL092W	*NUP145*	nuclear transportation	Y
YDR228C	*PCF11*	mRNA polyadenylylation	Y
YMR061W	*RNA14*	mRNA polyadenylylation	Y
YLR208W	*SEC13*	ER to Golgi vesicle-mediated transport	Y
YHR172W	*SPC97*	microtubule nucleation	Y
YGL207W	*SPT16*	chromatin remodeling & transcriptional regulation	Y
YLR212C	*TUB4*	microtubule nucleation	Y
YNL220W	*ADE12*	adenosine biosynthesis	N
YDR264C	*AKR1*	endocytosis	N
YDR035W	*ARO3*	aromatic amino acid family biosynthesis	N
YPR199C	*ARR1*	arsenite efflux	N
YPR201W	*ARR3*	arsenite efflux	N
YLR433C	*CNA1*	cell ion homeostasis & cell wall biogenesis	N
YLL009C	*COX17*	Intracellular copper ion transport	N
YBR112C	*CYC8*	chromatin remodeling & transcriptional regulation	N
YMR091C	*NPL6*	nuclear import & telomere maintenance	N
YER007W	*PAC2*	microtubule biogenesis	N
YPL159C	*PET20*	unknown	N
YDR300C	*PRO1*	proline biosynthesis	N
YOR265W	*RBL2*	microtubule biogenesis	N
YBR095C	*RXT2*	transcriptional regulation	N
YDR334W	*SWR1*	chromatin remodeling	N
YML124C	*TUB3*	microtubule biogenesis	N
YCR084C	*TUP1*	chromatin remodeling & transcriptional regulation	N
YBL086C	*YBL086C*	unknown	N

Note: [a] "Y" means that the gene is essential to yeast cell viability and "N" means that the gene is not essential. [b] "*YJL009W*" is a dubious ORF that overlaps with the ORF of *CCT8* required for protein folding.

TABLE S2

Arsenite-sensitive haploid YKOs

ORF Name	Gene Name	Biological Process	Arsenic sensitivity[a]	
			100 μM	400 μM
YNL153C	GIM3	actin & tubulin folding	SS	SS
YEL003W	GIM4	actin & tubulin folding	SS	SS
YML094W	GIM5	actin & tubulin folding	SS	SS
YGR078C	PAC10	actin & tubulin folding	SS	SS
YJL179W	PFD1	actin & tubulin folding	SS	SS
YLR200W	YKE2	actin & tubulin folding	SS	SS
YPL161C	BEM4	actin cytoskeleton organization and biogenesis	S	SS
YLR370C	ARC18	actin filament organization	NO	SS
YLR371W	ROM2	actin filament organization	SS	SS
YNL271C	BNI1	actin filament organization	NO	S
YNL084C	END3	actin filament organization; endocytosis	NO	SS
YJR125C	ENT3	actin filament organization; endocytosis	NO	S
YBR200W	BEM1	actin organization; establishment of cell polarity	NO	S
YPR199C	ARR1	arsenite detoxification	SS	SS
YPR201W	ARR3	arsenite detoxification	SS	SS
YDR135C	YCF1	arsenite detoxification	NO	SS
YFL023W	BUD27	bud site selection	SS	SS
YCR063W	BUD31	bud site selection	NO	SS
YKR061W	KTR2	cell wall mannoprotein biosynthesis	NO	S
YCR017C	CWH43	cell wall organization and biogenesis	NO	S
YDR293C	SSD1	cell wall organization and biogenesis	NO	SS
YLR085C	ARP6	chromatin remodeling; transcriptional regulation	NO	S
YOL012C	HTZ1	chromatin remodeling; transcriptional regulation	NO	SS
YOR304W	ISW2	chromatin remodeling; transcriptional regulation	NO	S
YNL192W	CHS1	cytokinesis	NO	S
YOL076W	MDM20	cytoskeleton organization and biogenesis	NO	S
YNL138W	SRV2	cytoskeleton organization and biogenesis	NO	SS
YDL101C	DUN1	DNA damage checkpoint	NO	S
YBL051C	PIN4	DNA damage checkpoint	NO	S
YER177W	BMH1	DNA damage checkpoint; cell polarization	NO	S
YLL002W	RTT109	DNA damage response; DNA transpotision	NO	S
YDL013W	HEX3	DNA repair	NO	S
YPR164W	MMS1	DNA repair	NO	S
YLR320W	MMS22	DNA repair	NO	SS
YMR224C	MRE11	DNA repair	NO	SS
YCR066W	RAD18	DNA repair	NO	S
YNL250W	RAD50	DNA repair	NO	S

YER095W	RAD51	DNA repair	NO	S
YML032C	RAD52	DNA repair	NO	SS
YGL163C	RAD54	DNA repair	NO	S
YDR004W	RAD57	DNA repair	NO	S
YJL047C	RTT101	DNA repair	NO	S
YHR154W	RTT107	DNA repair	NO	S
YER116C	SLX8	DNA repair	NO	S
YDR369C	XRS2	DNA repair	NO	SS
YJR043C	POL32	DNA repair; DNA replication	NO	S
YKL113C	RAD27	DNA repair; DNA replication	NO	SS
YJL115W	ASF1	DNA repair; histone assembly	NO	S
YGL058W	RAD6	DNA repair; histone ubiquitination & methylation	NO	S
YDL020C	RPN4	DNA repair; protein degradation	NO	S
YPR135W	CTF4	DNA repair; sister chromatid cohesion	NO	S
YHR191C	CTF8	DNA repair; sister chromatid cohesion	NO	S
YCL016C	DCC1	DNA repair; sister chromatid cohesion	NO	S
YGL127C	SOH1	DNA repair; transcriptional regulation	NO	S
YOR080W	DIA2	DNA replication	NO	S
YNR006W	VPS27	endosome transport	NO	S
YHR007C	ERG11	ergosterol biosynthesis	SS	SS
YMR202W	ERG2	ergosterol biosynthesis	NO	SS
YNL280C	ERG24	ergosterol biosynthesis	S	SS
YLR056W	ERG3	ergosterol biosynthesis	NO	S
YML008C	ERG6	ergosterol biosynthesis	NO	SS
YHR067W	RMD12	fatty acid biosynthesis	NO	S
YLR372W	SUR4	fatty acid biosynthesis	NO	SS
YLR087C	CSF1	fermentation	NO	SS
YGL084C	GUP1	glycerol transport	NO	S
YLR148W	PEP3	Golgi to endosome transport	NO	S
YMR231W	PEP5	Golgi to endosome transport	NO	S
YLR396C	VPS33	Golgi to endosome transport	NO	S
YER014W	HEM14	heme biosynthesis	S	SS
YCL010C	SGF29	histone acetylation	NO	S
YNL021W	HDA1	histone deacetylation	NO	S
YNL097C	PHO23	histone deacetylation	NO	S
YPR179C	PLO1	histone deacetylation	NO	S
YDR295C	PLO2	histone deacetylation	NO	S
YNL330C	RPD3	histone deacetylation	NO	SS
YMR263W	SAP30	histone deacetylation	NO	S
YIL084C	SDS3	histone deacetylation	NO	S
YOL004W	SIN3	histone deacetylation	NO	SS

YLR015W	BRE2	histone methylation	NO	S
YDR469W	SDC1	histone methylation	NO	S
YAR003W	SWD1	histone methylation	NO	S
YBR175W	SWD3	histone methylation	NO	S
YDL074C	BRE1	histone ubiquitination & methylation	NO	SS
YPL055C	LGE1	histone ubiquitination & methylation	NO	S
YMR077C	VPS20	late endosome to vacuole transport	NO	SS
YMR165C	PAH1	lipid biosynthesis	NO	SS
YOR349W	CIN1	microtubule biogenesis	NO	SS
YPL241C	CIN2	microtubule biogenesis	S	SS
YOR265W	RBL2	microtubule biogenesis	NO	SS
YML124C	TUB3	microtubule biogenesis	NO	SS
YDR150W	NUM1	microtubule organization and biogenesis	NO	S
YHR129C	ARP1	microtubule-mediated nuclear migration	NO	S
YER016W	BIM1	microtubule-mediated nuclear migration	NO	S
YMR294W	JNM1	microtubule-mediated nuclear migration	NO	S
YDR488C	PAC11	microtubule-mediated nuclear migration	NO	S
YJR118C	ILM1	mitochondrial genome maintenance	NO	SS
YHR038W	FIL1	mitochondrion protein biosynthesis	NO	SS
YPR120C	CLB5	mitotic cell cycle (G1/S and G2/M transition)	NO	S
YER167W	BCK2	mitotic cell cycle (G1/S transition)	NO	S
YFR040W	SAP155	mitotic cell cycle (G1/S transition)	NO	S
YLR079W	SIC1	mitotic cell cycle (G1/S transition)	NO	S
YPR119W	CLB2	mitotic cell cycle (G2/M transition)	NO	S
YFR036W	CDC26	mitotic cell cycle (metaphase/anaphase transition)	SS	SS
YAL024C	LTE1	mitotic cell cycle (mitotic exit)	S	SS
YNL298W	CLA4	mitotic cell cycle (mitotic exit); cell polarization	NO	SS
YPL008W	CHL1	mitotic sister chromatid cohesion	NO	S
YOR073W	SGO1	mitotic spindle checkpoint	NO	S
YEL061C	CIN8	mitotic spindle organization and biogenesis	NO	S
YCR065W	HCM1	mitotic spindle organization and biogenesis	NO	S
YIL153W	RRD1	mitotic spindle organization and biogenesis	NO	S
YGL094C	PAN2	mRNA 3'-end processing; DNA repair	NO	S
YDR497C	ITR1	myo-inositol transport	NO	S
YOR371C	GPB1	negative regulation of cAMP signalling	NO	S
YAL056W	GPB2	negative regulation of cAMP signalling	NO	S
YBR140C	IRA1	negative regulation of cAMP signalling	NO	S
YOL081W	IRA2	negative regulation of cAMP signalling	S	SS
YOR360C	PDE2	negative regulation of cAMP signalling	NO	S
YHR013C	ARD1	N-terminal protein amino acid acetylation	NO	SS
YEL053C	MAK10	N-terminal protein amino acid acetylation	NO	S

YDL040C	NAT1	N-terminal protein amino acid acetylation	S	SS
YLR293C	GSP1	nucleocytoplasmic transport	S	SS
YLR113W	HOG1	osmotic stress response; regulation of arsenic uptake	NO	SS
YLR006C	SSK1	osmotic stress response; regulation of arsenic uptake	NO	SS
YNR031C	SSK2	osmotic stress response; regulation of arsenic uptake	NO	SS
YJL128C	PBS2	osmotic stress response; regulation of arsenic uptake	NO	SS
YMR038C	LYS7	oxidative stress response	S	SS
YNL099C	OCA1	oxidative stress response	NO	S
YHR206W	SKN7	oxidative stress response	NO	S
YJR104C	SOD1	oxidative stress response	SS	SS
YML028W	TSA1	oxidative stress response	NO	S
YML007W	YAP1	oxidative stress response	NO	SS
YCR028C	FEN2	pantothenate transport	NO	SS
YKL197C	PEX1	peroxisome organization and biogenesis	NO	S
YDR265W	PEX10	peroxisome organization and biogenesis	NO	S
YLR191W	PEX13	peroxisome organization and biogenesis	NO	S
YGL153W	PEX14	peroxisome organization and biogenesis	NO	S
YOL044W	PEX15	peroxisome organization and biogenesis	NO	S
YNL214W	PEX17	peroxisome organization and biogenesis	NO	S
YDL065C	PEX19	peroxisome organization and biogenesis	NO	S
YJL210W	PEX2	peroxisome organization and biogenesis	NO	S
YAL055W	PEX22	peroxisome organization and biogenesis	NO	S
YDR329C	PEX3	peroxisome organization and biogenesis	NO	S
YGR133W	PEX4	peroxisome organization and biogenesis	NO	SS
YDR244W	PEX5	peroxisome organization and biogenesis	NO	S
YNL329C	PEX6	peroxisome organization and biogenesis	NO	SS
YGR077C	PEX8	peroxisome organization and biogenesis	NO	S
YJR073C	OPI3	phosphatidylcholine biosynthesis	NO	S
YHL020C	OPI1	phospholipid biosynthesis	NO	S
YGR123C	PPT1	protein amino acid dephosphorylation	NO	S
YJL183W	MNN11	protein amino acid glycosylation	S	SS
YGL038C	OCH1	protein amino acid N-linked glycosylation	NO	SS
YML115C	VAN1	protein amino acid N-linked glycosylation	NO	SS
YOR124C	UBP2	protein deubiquitination	NO	SS
YPL106C	SSE1	protein folding	NO	S
YER110C	KAP123	protein import into nucleus	NO	S
YBR171W	SEC66	protein targeting to membrane	NO	S
YCL008C	STP22	protein targeting to membrane	NO	S
YPL084W	BRO1	protein targeting to vacuole	NO	SS
YPL002C	SNF8	protein targeting to vacuole	NO	SS
YJR102C	VPS25	protein targeting to vacuole	S	SS

YLR417W	VPS36	protein targeting to vacuole	S	SS
YDR136C	VPS61	protein targeting to vacuole	NO	SS
YNL297C	MON2	protein targeting to vacuole; endocytosis	NO	SS
YKL176C	LST4	protein transport Golgi to plasma membrane	NO	SS
YGR057C	LST7	protein transport Golgi to plasma membrane	NO	SS
YMR275C	BUL1	protein ubiquitination	S	SS
YPL139C	UME1	regulation of meiosis	NO	S
YNL229C	URE2	regulation of nitrogen utilization	NO	S
YNL201C	PSY2	response to drug	NO	S
YER083C	GET2	retrograde vesicle-mediated transport	NO	S
YFL001W	DEG1	RNA processing	S	SS
YML016C	PPZ1	sodium ion homeostasis	NO	SS
YDR001C	NTH1	Stress response	NO	S
YNL307C	MCK1	Stress response; DNA repair	NO	SS
YAL012W	CYS3	sulfur amino acid metabolism	S	SS
YOL138C	YOL138C	telomere maintenance	NO	SS
YDR195W	REF2	transcriptional regulation	NO	SS
YBR095C	RXT2	transcriptional regulation	NO	S
YNL236W	SIN4	transcriptional regulation	NO	S
YDR463W	STP1	transcriptional regulation	NO	S
YBL024W	NCL1	tRNA methylation	NO	S
YDR525W	API2	unknown	NO	S
YLR338W	OPI9	unknown	S	SS
YBL104C	YBL104C	unknown	NO	SS
YCR082W	YCR082W	unknown	NO	S
YJL120W	YJL120W	unknown	NO	SS
YKL097C	YKL097C	unknown	NO	S
YLL049W	YLL049W	unknown	NO	S
YPL066W	YPL066W	unknown	NO	S
YLR373C	VID22	vacuolar protein catabolism	NO	SS
YNL054W	VAC7	vacuole inheritance and morphology	NO	S

Note: [a] Individual haploid-convertible heterozygote diploid YKOs were sporulated and spotted at 10 x serial dilution on solid haploid selection magic medium in the presence of sodium arsenite at indicated concentrations. Growth of each strain was compared to an isogenic *ho*Δ mutant, which acts as a surrogate wild-type strain. "SS", the mutant was hypersensitive to the drug at indicated concentration; "S", modestly sensitive; "NO", not sensitive. YKOs of dubious ORFs that overlap with known genes were excluded from this table. These include *yml094c-a*Δ, which is deleted for part of *GIM5* and was one of the nine most arsenic-sensitive YKOs.

TABLE S3

Arsenic-resistant haploid YKOs

ORF Name	Gene name	Biological Process
YLR410W	VIP1	actin cytoskeleton organization and biogenesis
YLL043W	FPS1	arsenite uptake
YCR047C	BUD23	bud site selection
YGR221C	TOS2	budding cell bud growth
YJL184W	YJL184W	cell wall mannoprotein biosynthesis
YLR110C	CCW12	cell wall organization and biogenesis
YIL085C	KTR7	cell wall organization and biogenesis
YNL227C	JJJ1	endocytosis
YGL054C	ERV14	ER to Golgi vesicle-mediated transport
YIR026C	YVH1	glycogen metabolism
YKR042W	UTH1	mitochondrion organization and biogenesis
YGL019W	CKB1	mitotic cell cycle; ion homeostasis
YOR039W	CKB2	mitotic cell cycle; ion homeostasis
YKR072C	SIS2	mitotic cell cycle; salt stress response
YDR432W	NPL3	mRNA export from nucleus
YDR378C	LSM6	mRNA splicing
YMR080C	NAM7	nonsense-mediated mRNA decay
YHR077C	NMD2	nonsense-mediated mRNA decay
YGR072W	UPF3	nonsense-mediated mRNA decay
YDR140W	MTQ2	peptidyl-glutamine methylation
YOR085W	OST3	protein amino acid glycosylation
YDL081C	RPP1A	protein biosynthesis
YDR382W	RPP2B	protein biosynthesis
YLR192C	HCR1	protein biosynthesis; ribosomal RNA processing
YGR085C	RPL11B	protein biosynthesis; structural constituent of ribosome
YDR418W	RPL12B	protein biosynthesis; structural constituent of ribosome
YDL082W	RPL13A	protein biosynthesis; structural constituent of ribosome
YMR142C	RPL13B	protein biosynthesis; structural constituent of ribosome
YKL006W	RPL14A	protein biosynthesis; structural constituent of ribosome
YNL069C	RPL16B	protein biosynthesis; structural constituent of ribosome
YBL027W	RPL19B	protein biosynthesis; structural constituent of ribosome
YGL135W	RPL1B	protein biosynthesis; structural constituent of ribosome
YMR242C	RPL20A	protein biosynthesis; structural constituent of ribosome
YOR312C	RPL20B	protein biosynthesis; structural constituent of ribosome
YBR191W	RPL21A	protein biosynthesis; structural constituent of ribosome
YLR061W	RPL22A	protein biosynthesis; structural constituent of ribosome
YER117W	RPL23B	protein biosynthesis; structural constituent of ribosome
YGL031C	RPL24A	protein biosynthesis; structural constituent of ribosome

YIL052C	RPL34B	protein biosynthesis; structural constituent of ribosome
YDL191W	RPL35A	protein biosynthesis; structural constituent of ribosome
YLR185W	RPL37A	protein biosynthesis; structural constituent of ribosome
YJL189W	RPL39	protein biosynthesis; structural constituent of ribosome
YKR094C	RPL40B	protein biosynthesis; structural constituent of ribosome
YPR043W	RPL43A	protein biosynthesis; structural constituent of ribosome
YBR031W	RPL4A	protein biosynthesis; structural constituent of ribosome
YML073C	RPL6A	protein biosynthesis; structural constituent of ribosome
YLR448W	RPL6B	protein biosynthesis; structural constituent of ribosome
YGL076C	RPL7A	protein biosynthesis; structural constituent of ribosome
YHL033C	RPL8A	protein biosynthesis; structural constituent of ribosome
YNL067W	RPL9B	protein biosynthesis; structural constituent of ribosome
YLR048W	RPS0B	protein biosynthesis; structural constituent of ribosome
YOR293W	RPS10A	protein biosynthesis; structural constituent of ribosome
YDR025W	RPS11A	protein biosynthesis; structural constituent of ribosome
YBR048W	RPS11B	protein biosynthesis; structural constituent of ribosome
YMR143W	RPS16A	protein biosynthesis; structural constituent of ribosome
YDL083C	RPS16B	protein biosynthesis; structural constituent of ribosome
YML024W	RPS17A	protein biosynthesis; structural constituent of ribosome
YDR450W	RPS18A	protein biosynthesis; structural constituent of ribosome
YML026C	RPS18B	protein biosynthesis; structural constituent of ribosome
YNL302C	RPS19B	protein biosynthesis; structural constituent of ribosome
YLR441C	RPS1A	protein biosynthesis; structural constituent of ribosome
YML063W	RPS1B	protein biosynthesis; structural constituent of ribosome
YJL136C	RPS21B	protein biosynthesis; structural constituent of ribosome
YGR118W	RPS23A	protein biosynthesis; structural constituent of ribosome
YPR132W	RPS23B	protein biosynthesis; structural constituent of ribosome
YER074W	RPS24A	protein biosynthesis; structural constituent of ribosome
YHR021C	RPS27B	protein biosynthesis; structural constituent of ribosome
YLR264W	RPS28B	protein biosynthesis; structural constituent of ribosome
YDL061C	RPS29B	protein biosynthesis; structural constituent of ribosome
YOR182C	RPS30B	protein biosynthesis; structural constituent of ribosome
YJR145C	RPS4A	protein biosynthesis; structural constituent of ribosome
YHR203C	RPS4B	protein biosynthesis; structural constituent of ribosome
YPL090C	RPS6A	protein biosynthesis; structural constituent of ribosome
YBR181C	RPS6B	protein biosynthesis; structural constituent of ribosome
YOR096W	RPS7A	protein biosynthesis; structural constituent of ribosome
YBL072C	RPS8A	protein biosynthesis; structural constituent of ribosome
YBR189W	RPS9B	protein biosynthesis; structural constituent of ribosome
YPL125W	KAP120	protein import into nucleus
YDR414C	ERD1	protein retention in ER

YML106W	URA5	pyrimidine base biosynthesis
YPL268W	PLC1	regulation of phosphate metabolism
YKR024C	DBP7	ribosomal large subunit assembly and maintenance
YPL193W	RSA1	ribosomal large subunit assembly and maintenance
YFR001W	LOC1	ribosomal large subunit biogenesis
YBR267W	REI1	ribosomal large subunit biogenesis
YLR068W	FYV7	ribosomal RNA processing
YOL041C	NOP12	ribosomal RNA processing
YGR159C	NSR1	ribosomal RNA processing
YGL246C	RAI1	ribosomal RNA processing
YOR001W	RRP6	ribosomal RNA processing
YHR081W	LRP1	ribosomal RNA processing; snoRNA processing
YKL143W	LTV1	ribosomal small subunit biogenesis; stress response
YPL239W	YAR1	ribosomal small subunit biogenesis; stress response
YLR418C	CDC73	transcriptional regulation
YMR136W	GAT2	transcriptional regulation
YOR123C	LEO1	transcriptional regulation
YLR131C	ACE2	transcriptional regulation specific in G1 phase
YIL128W	MET18	transcriptional regulation; methionine metabolism
YGR097W	ASK10	transcriptional regulation; oxidative stress response
YBL067C	UBP13	unknown
YDL063C	YDL063C	unknown
YDR161W	YDR161W	unknown
YGR131W	YGR131W	unknown
YLR111W	YLR111W	unknown
YLR184W	YLR184W	unknown
YOR309C	YOR309C	unknown
YDR349C	YPS7	unknown
YEL062W	NPR2	urea and L-proline transport
YDR017C	KCS1	vacuole organization and biogenesis

Note: Individual haploid-convertible heterozygote diploid YKOs were sporulated and spotted at 10 x serial dilution on solid haploid selection magic medium in the presence of 1 mM of sodium arsenite, which almost completely inhibits growth of an isogenic *ho*Δ mutant (as control). Strains grew in this medium were scored as resistant and listed here. YKOs of dubious ORFs that overlap with known genes were excluded from this table.

TABLE S4

Arsenite-hypersensitivity of *pfd1*Δ-related double mutants.

ORF Name	Gene Name	Synthetic interaction with *pfd1*Δ*::URA3*	
		-As(III)	5 μM As(III)
YBR231C	*AOR1*	SL	SL
YLR085C	*ARP6*	SL	SL
YOR026W	*BUB3*	SL	SL
YOR349W	*CIN1*	SL	SL
YPL241C	*CIN2*	SL	SL
YEL061C	*CIN8*	SL	SL
YKL139W	*CTK1*	SL	SL
YML112W	*CTK3*	SL	SL
YNL084C	*END3*	SL	SL
YNL133C	*FYV6*	SL	SL
YML128C	*MSC1*	SL	SL
YOR265W	*RBL2*	SL	SL
YOR073W	*SGO1*	SL	SL
YBL058W	*SHP1*	SL	SL
YLR025W	*SNF7*	SL	SL
YPR101W	*SNT309*	SL	SL
YML124C	*TUB3*	SL	SL
YNL054W	*VAC7*	SL	SL
YNL107W	*YAF9*	SL	SL
YCR064C	*YCR064C*	SL	SL
YLR338W	*YLR338W*	SL	SL
YMR074C	*YMR074C*	SL	SL
YLR370C	*ARC18*	SF/SL	SL
YER016W	*BIM1*	SF/SL	SL
YJL006C	*CTK2*	SF/SL	SL
YOL012C	*HTZ1*	SF/SL	SL
YAL024C	*LTE1*	SF/SL	SL
YGL094C	*PAN2*	SF/SL	SL
YKL025C	*PAN3*	SF/SL	SL
YDL020C	*RPN4*	SF/SL	SL
YOR035C	*SHE4*	SF/SL	SL
YMR179W	*SPT21*	SF/SL	SL
YNL138W	*SRV2*	SF/SL	SL
YDR334W	*SWR1*	SF/SL	SL
YOR332W	*VMA4*	SF/SL	SL

YEL051W	*VMA8*	SF/SL	SL
YCL029C	*BIK1*	SF/SL	SF/SL
YIL036W	*CST6*	SF/SL	SF/SL
YNL148C	*ALF1*	SF	SL
YMR138W	*CIN4*	SF	SL
YNL298W	*CLA4*	SF	SL
YNR010W	*CSE2*	SF	SL
YEL027W	*CUP5*	SF	SL
YJR118C	*ILM1*	SF	SL
YPR141C	*KAR3*	SF	SL
YEL053C	*MAK10*	SF	SL
YOL076W	*MDM20*	SF	SL
YNL297C	*MON2*	SF	SL
YPL226W	*NEW1*	SF	SL
YDR488C	*PAC11*	SF	SL
YOR266W	*PNT1*	SF	SL
YNL180C	*RHO5*	SF	SL
YCR009C	*RVS161*	SF	SL
YCL037C	*SRO9*	SF	SL
YLR447C	*VMA6*	SF	SL
YKL037W	*YKL037W*	SF	SL
YLR358C	*YLR358C*	SF	SL
YNL140C	*YNL140C*	SF	SL
YHR129C	*ARP1*	SF	SF/SL
YCL016C	*DCC1*	SF	SF/SL
YMR294W	*JNM1*	SF	SF/SL
YKR061W	*KTR2*	SF	SF/SL
YMR038C	*LYS7*	SF	SF/SL
YHR194W	*MDM31*	SF	SF/SL
YPL174C	*NIP100*	SF	SF/SL
YDR150W	*NUM1*	SF	SF/SL
YML061C	*PIF1*	SF	SF/SL
YHR026W	*PPA1*	SF	SF/SL
YDL006W	*PTC1*	SF	SF/SL
YOR014W	*RTS1*	SF	SF/SL
YPL002C	*SNF8*	SF	SF/SL
YCL008C	*STP22*	SF	SF/SL
YGR020C	*VMA7*	SF	SF/SL
YJR102C	*VPS25*	SF	SF/SL
YLR417W	*VPS36*	SF	SF/SL

YDR149C	*YDR149C*	SF	SF/SL
YER177W	*BMH1*	SF	SF
YCR086W	*CSM1*	SF	SF
YPR023C	*EAF3*	SF	SF
YGL086W	*MAD1*	SF	SF
YJL030W	*MAD2*	SF	SF
YPR199C	*ARR1*	NO	SL
YPR201W	*ARR3*	NO	SL
YDL115C	*IWR1*	NO	SL
YPR051W	*MAK3*	NO	SL
YPL118W	*MRP51*	NO	SL
YBL024W	*NCL1*	NO	SL
YDR176W	*NGG1*	NO	SL
YJR104C	*SOD1*	NO	SL
YPL129W	*TAF14*	NO	SL
YBR097W	*VPS15*	NO	SL
YDR525W	*API2*	NO	SF/SL
YJR053W	*BFA1*	NO	SF/SL
YJR060W	*CBF1*	NO	SF/SL
YLR087C	*CSF1*	NO	SF/SL
YML008C	*ERG6*	NO	SF/SL
YML006C	*GIS4*	NO	SF/SL
YGL084C	*GUP1*	NO	SF/SL
YLL026W	*HSP104*	NO	SF/SL
YGL253W	*HXK2*	NO	SF/SL
YLR099C	*ICT1*	NO	SF/SL
YBR107C	*IML3*	NO	SF/SL
YLR095C	*IOC2*	NO	SF/SL
YER110C	*KAP123*	NO	SF/SL
YPR046W	*MCM16*	NO	SF/SL
YDR318W	*MCM21*	NO	SF/SL
YDR162C	*NBP2*	NO	SF/SL
YNL097C	*PHO23*	NO	SF/SL
YML032C	*RAD52*	NO	SF/SL
YNL330C	*RPD3*	NO	SF/SL
YLL002W	*RTT109*	NO	SF/SL
YDR388W	*RVS167*	NO	SF/SL
YOL004W	*SIN3*	NO	SF/SL
YNL167C	*SKO1*	NO	SF/SL
YGR229C	*SMI1*	NO	SF/SL

YDR293C	*SSD1*	NO	SF/SL
YPL253C	*VIK1*	NO	SF/SL
YHR012W	*VPS29*	NO	SF/SL
YML007W	*YAP1*	NO	SF/SL
YHL029C	*YHL029C*	NO	SF/SL
YML081W	*YML081W*	NO	SF/SL
YNL326C	*YNL326C*	NO	SF/SL
YPR200C	*ARR2*	NO	SF
YFL025C	*BST1*	NO	SF
YDR252W	*BTT1*	NO	SF
YMR055C	*BUB2*	NO	SF
YGL003C	*CDH1*	NO	SF
YPL008W	*CHL1*	NO	SF
YDR254W	*CHL4*	NO	SF
YJL158C	*CIS3*	NO	SF
YBR036C	*CSG2*	NO	SF
YMR048W	*CSM3*	NO	SF
YJR084W	*CSN12*	NO	SF
YPL018W	*CTF19*	NO	SF
YLR381W	*CTF3*	NO	SF
YHR191C	*CTF8*	NO	SF
YMR264W	*CUE1*	NO	SF
YDR480W	*DIG2*	NO	SF
YKR054C	*DYN1*	NO	SF
YDR424C	*DYN2*	NO	SF
YNL106C	*INP52*	NO	SF
YER019W	*ISC1*	NO	SF
YJL062W	*LAS21*	NO	SF
YNL268W	*LYP1*	NO	SF
YJL013C	*MAD3*	NO	SF
YDL056W	*MBP1*	NO	SF
YJR135C	*MCM22*	NO	SF
YMR224C	*MRE11*	NO	SF
YNL053W	*MSG5*	NO	SF
YOL116W	*MSN1*	NO	SF
YMR109W	*MYO5*	NO	SF
YNL183C	*NPR1*	NO	SF
YNL099C	*OCA1*	NO	SF
YJL128C	*PBS2*	NO	SF
YKL127W	*PGM1*	NO	SF

YBR092C	*PHO3*	NO	SF
YBL051C	*PIN4*	NO	SF
YDR075W	*PPH3*	NO	SF
YMR137C	*PSO2*	NO	SF
YNL250W	*RAD50*	NO	SF
YER095W	*RAD51*	NO	SF
YNL098C	*RAS2*	NO	SF
YDL189W	*RBS1*	NO	SF
YMR075W	*RCO1*	NO	SF
YDR289C	*RTT103*	NO	SF
YBR171W	*SEC66*	NO	SF
YLR292C	*SEC72*	NO	SF
YMR216C	*SKY1*	NO	SF
YGL127C	*SOH1*	NO	SF
YER161C	*SPT2*	NO	SF
YLR119W	*SRN2*	NO	SF
YLR006C	*SSK1*	NO	SF
YNR031C	*SSK2*	NO	SF
YBR118W	*TEF2*	NO	SF
YNL273W	*TOF1*	NO	SF
YJL129C	*TRK1*	NO	SF
YKR056W	*TRM2*	NO	SF
YOR344C	*TYE7*	NO	SF
YDL190C	*UFD2*	NO	SF
YNL229C	*URE2*	NO	SF
YLR386W	*VAC14*	NO	SF
YGL212W	*VAM7*	NO	SF
YNR006W	*VPS27*	NO	SF
YOR083W	*WHI5*	NO	SF
YBR042C	*YBR042C*	NO	SF
YBR232C	*YBR232C*	NO	SF
YCR082W	*YCR082W*	NO	SF
YDL146W	*YDL146W*	NO	SF
YDL211C	*YDL211C*	NO	SF
YER139C	*YER139C*	NO	SF
YGL060W	*YGL060W*	NO	SF
YGR117C	*YGR117C*	NO	SF
YJL120W	*YJL120W*	NO	SF
YJL169W	*YJL169W*	NO	SF
YJR119C	*YJR119C*	NO	SF

YJR129C	*YJR129C*	NO	SF
YLL049W	*YLL049W*	NO	SF
YLR278C	*YLR278C*	NO	SF
YMR144W	*YMR144W*	NO	SF
YMR160W	*YMR160W*	NO	SF
YMR160W	*YMR160W*	NO	SF
YMR247C	*YMR247C*	NO	SF
YNL056W	*YNL056W*	NO	SF
YNL116W	*YNL116W*	NO	SF
YNR009W	*YNR009W*	NO	SF
YOR019W	*YOR019W*	NO	SF
YOR291W	*YOR291W*	NO	SF
YPL017C	*YPL017C*	NO	SF
YNR039C	*ZRG17*	NO	SF

Note: Haploid-convertible heterozygote diploid YKOs of listed genes were individually transformed with a *pfd1*Δ*::URA3* query construct to create heterozygote double mutants, which were subsequently sporulated and spotted at 10 x serial dilution onto different haploid selection magic media (MM). To verify synthetic lethality interactions between the listed gene mutations and *pfd1*Δ, MM lacking uracil was used to select for the *xxx*Δ*::kanMX pfd1*Δ*::URA3* double mutants, MM for the *xxx*Δ*::kanMX* single and *xxx*Δ*::kanMX pfd1*Δ*::URA3* double mutants, and MM lacking both uracil and G418 for the *pfd1*Δ*::URA3* single and *xxx*Δ*::kanMX pfd1*Δ*::URA3* double mutants. ("*xxx*" stands for mutation of any gene listed.) 5 μM of sodium arsenite, which had no obvious effect on any single mutant, was either included or excluded. The genetic interactions were scored as SF (modest synthetic fitness defect), SF/SL (severe synthetic fitness defect), SL (synthetic lethality), or NO (no synthetic interaction).